Biomonitoring and Source Identification of Polycyclic Aromatic Hydrocarbons (PAHs) Using Pine Tree Components from Three Different Sites in Bursa, Turkey

Mehmet Ferhat Sari[1] · Fatma Esen[1] · Yücel Tasdemir[1]

Abstract

Pine trees are used as biomonitoring agents to evaluate atmospheric polycyclic aromatic hydrocarbons (PAHs). Due to industrialization, urban construction, and rapid population growth, the city of Bursa is experiencing air pollution. In this study, PAHs were measured in pine tree branches and needles at a wastewater treatment plant site, an industrial site, and semirural site in Bursa for 12 months. The concentrations fluctuated depending on the characteristics of the areas. The lowest concentration value was measured in the semirural site while the highest value was determined in the wastewater treatment plant site. The PAH concentrations in pine needles ranged from 24 to 2565 ng/g dry weight (DW) and in pine branches from 163 to 2871 ng/g DW for 16 PAHs. Naphthalene, phenanthrene, fluorene, and fluoranthene were determined as dominant species in both tree components. Diagnostic ratios, ring profile, principal component analysis, the coefficient of divergence, and the Pearson correlation coefficient methods were used in the definition of sources of PAHs in the sampling sites, although all source identification methods have advantages and disadvantages. According to the results, the PAHs mainly originated from biomass and coal burning, traffic, and mixed sources. It also was concluded that three sampling sites showed higher PAH concentrations during winter, and the main PAH sources were similar.

The increase of motor vehicles, industrial establishments, and urbanization significantly disrupts the quality of ambient air in urban areas where the population is high (Taghvaee et al. 2018). Polycyclic aromatic hydrocarbons (PAHs) are mainly given from the incomplete combustion of fossil fuels, from oil spills, and from industrial processes to the atmosphere and cause it to spread to the atmosphere (Ozaki et al. 2015). Among the important PAH sources in wastewater treatment plants to be treated are wastewater, pipe and tank coatings, running water, air, and wastewater from human activities (Torretta 2012). Also, biodegradation, volatilization, and adsorption are considered among the methods used to remove PAHs from wastewater treatment plants (Liu et al.

✉ Yücel Tasdemir
    tasdemir@uludag.edu.tr

[1] Department of Environmental Engineering, Faculty of Engineering, Bursa Uludag University, 16059 Nilüfer, Bursa, Turkey

2011). The air-water exchange of PAHs is an important process that determines the transport and fate of these pollutants between the atmosphere and large water bodies (Fang et al. 2012). PAHs are usually released during the combustion of organic matter. Intensive industries, such as iron and steel, cement, and energy production are listed as key industries for controlling atmospheric PAHs (Li et al. 2013). In the study conducted by Nguyen et al. (2018) in South Korea, PAH sources are mainly produced in semiurban regions due to petrochemical and nonferrous activities, aluminum production, and other processes (Nguyen et al. 2018).

The amount of PAH accumulated in plants depends on different factors, such as external pollution level, exposure time, and morphological and physiological characteristics of the species studied (Malawska et al. 2006; Oishi 2013; Mętrak et al. 2016). Conifers, having many types, are commonly found in the environment. Several studies have shown that the leaves of conifers were good and reliable indicators for organic and inorganic air pollutants (Piccardo et al. 2005; Mętrak et al. 2016). Pollutants in the gaseous phase can penetrate directly from the pores into the interior of the leaves or they can spread through the candle on the cuticle (Howsam et al. 2000; Lehndorff and Schwark 2004). PAHs absorbed

by the leaves do not reach equilibrium and show back diffusion or degradation (Lehndorff and Schwark 2004). Some of the PAHs that accumulate on the leaves and are connected to the particles are separated from the surface of the leaves by wind and rainfall, but a large part of them enters the candle cover (Lehndorff and Schwark 2004).

The most important anthropogenic sources of PAHs are the incomplete combustion of hydrocarbons, such as coal, oil, wood, and petroleum products (Dat and Chang 2017). The identification of emission sources of total PAH concentrations in ambient air is usually performed using diagnostic ratios (DRs) or receptor models (Agudelo-Castañeda and Teixeira 2014). Different DRs are used for the determination of PAH emissions as a result of the sources of petrogenic, pyrolytic, and combustion of biomass and coal (Duodu et al. 2017). Specifically, the general principle of establishing a DR is to determine a homologous group in terms of molecular weight or aromatic ring number distributions and to minimize the differences between the boiling point, vapor pressure, octanol-water partition coefficient, and water solubility of the PAHs within the designated homolog group (Cheng et al. 2019). Statistical tools, such as principal component analysis (PCA), also are used to identify PAH sources. PCA is a statistical analysis method that converts a few important explanatory factors or key principal components (PCs) that emphasize the most important information of a data set (Nguyen et al. 2018).

Pine tree branch and needle samples were collected between January and December 2016 from different regions, including a semirural site, an industrial site, and a wastewater treatment plant for analyzing PAHs. The purpose of this study was (1) to determine the levels of PAH compounds in tree components, (2) to show the temporal changes of PAH concentrations, and (3) to identify the sources of PAHs by introducing multiple methods.

Material and Methods

Sampling

The pine tree branch and needle samples from three different sites were collected monthly between January and December 2016 in Bursa. Samples were collected from a semirural site (SRS; 40°19′49.60″N–28°53′50.80″E), an industrial site (IS; 40°25′24.30″N–29°16′12.67″E), and a wastewater treatment plant site (WWTPS; 40°13′50.10″N–29°4′58.25″E) (Fig. 1). To represent the whole tree, the samples were taken homogeneously from different points of the tree. To avoid any contamination of the samples during transportation to the laboratory, they were packaged in aluminum foil and put in the sealed bags without contact with air and kept in – 20 °C freezer until they were prepared for analysis.
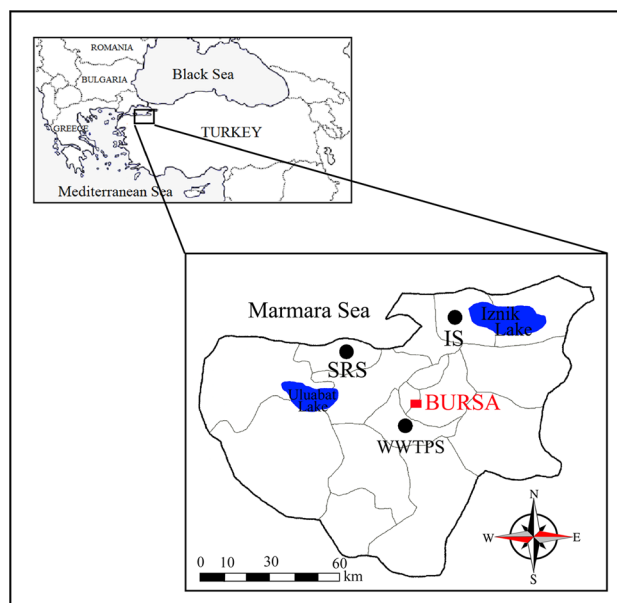

Fig. 1 Sampling sites

Sample Preparation and Analysis

Approximately 5 g of each of the pine tree branch and needle samples were weighed and cut into small pieces and then taken into amber bottles separately. After adding 50 mL of Petroleum Ether: Dichloromethane (PE:DCM) (1:1) solution on each of the samples, 1 mL of the surrogate standard was added to determine the recovery efficiencies. Bottles, including samples, were placed on the shaker for 24 h (Esen et al. 2006; Tasdemir and Esen 2007). After the shaker, the amber bottles containing the sample solutions were placed into an ultrasonic extraction device (Elmasonic S80 (H), Germany). The extraction was performed in two steps: the sample was first extracted for 15 min and drained to another flask, and then 40 mL of Acetone:Hexane (ACE:HEX) (1:1 v:v) mixture was added to the sample and extracted for another 30 min in the ultrasonic extraction. The rotary evaporator (Laborota 4001 Model, Heidolph, Germany) was used to reduce the volume of the solution. The volume of the mixture was reduced to 5 mL in a rotary evaporator operating at 30 rpm and 22 °C. Then, 15 mL of HEX was added and reduced to 2 mL. In this step, the solvent was exchanged to HEX. The 2-mL sample was fractionated by using 3 g of silicic acid (3% pure water), 2 g of alumina (6% pure water), and 2 g of sodium sulfate (Na_2SO_4) (Günindi and Tasdemir 2010; Kuzu 2016). The column was first purged with 20 mL of DCM followed by 20 mL of PE. Then, 2 mL of the sample was passed through the column, and 20 mL of PE was passed to collect the PCBs. After that,

20 mL DCM was passed, and PAHs were collected in a different flask placed under the column (Vardar et al. 2004; Tasdemir and Esen 2007). The volume of collected PAH solutions was reduced to 5 mL with the aid of a rotary evaporator, and 10 mL of HEX was added to ensure the solvent exchange. The sample was finally reduced to 1 mL and vialed. Sample vials were kept in the freezer at −20 °C until gas chromatograph (GC) readings.

The analysis of PAHs was performed by Agilent 7890A model GC with an Agilent 5975C model mass spectrophotometer (MS). A capillary column (HP 5-MS, 30 m × 250 μm × 0.25 μm) was used in the GC-MS. The oven temperature program was 50 °C (2 min), with increases of 25 °C/min up to 200 °C, followed by 3 °C/min up to 300 °C (5.5 min), then 5 °C/min up to 310 °C (3 min). The injector inlet temperature was 250 °C, and the detector temperature was 320 °C. Retention times and intended ion peak values were taken into account for the determination of PAH compounds. In this study, 16 PAH compounds were targeted: Naphthalene (NAP), Acenaphthylene (ACE), Acenaphthene (ACT), Fluorene (FLN), Phenanthrene (PHE), Anthracene (ANT), Fluoranthene (FL), Pyrene (PY), benz(a) anthracene (BaA), Chrysene (CHR), Benzo(b)flouranthene (BbF), Benzo(k)fluoranthene (BkF), Benzo(a)pyrene (BaP), Indeno(1,2,3-cd)pyren (IcdP), Dibenz[a,h]anthracene (DahA), and Benzo(g,h,i)perylene (BghiP). Specific ions used in the quantitative analysis of PAHs by GC-MS for each PAH compound are presented in Table S1 (Supplementary material).

Software Package

In this study, the Pearson correlation coefficients (PCCs) were calculated with the Statistical Package for the Social Sciences® (SPSS) version 23.0. The coefficient of divergences (CODs) was also achieved with the Microsoft Excel® (2016), and all figures were constructed with the SigmaPlot® version 13.0.

Quality Assurance/Quality Control (QA/QC)

The GC-MS was calibrated before determining the mass values in the samples. Six levels of calibration standards (0.04, 0.4, 1.0, 4.0, 6.0, 10.0 μg/mL) were used for this purpose. For all calibration levels, the r^2 values were calculated to be greater than 0.99. In addition, a medium level calibration standard (1.0 or 4.0 μg/mL) was read in every 100 samples, and the calibration requirement of GC-MS was determined. Targeted PAH compounds were checked for their retention times and mass readings. When any PAH compound showed approximately 10% fluctuation, a new calibration was achieved. Samples with recovery efficiencies between 40 and 120% were taken into account in the calculations.

For the determination of the analytical recovery efficiencies of the samples, a standard of surrogate consisting of naphthalene-d8, acenaphthene-d10, phenanthrene-d10, chrysene-d12, and perylene-d12 at a concentration of 4 μg/mL was added to the samples before extraction.

To eliminate the effects of possible contamination on the reported values, the blank correction was applied by subtracting the mean of the blank values for each PAH compound from the values obtained from the samples (Cindoruk et al. 2005; Esen et al. 2008). In addition, the limit of detection (LOD) values obtained by using the blank samples were taken into account in the calculations. LOD values were calculated for each measured compound as an average mass in blank plus three times the standard deviation (average + 3 SD). Measured sample values smaller than LOD were not included in the calculations (Tasdemir and Esen 2007; Ozcan and Aydin 2009).

Results and Discussion

PAH Concentrations in the Pine Branches and Pine Needles

In this study, pine branches and needles from the regions representing different environments [semi-rural (SRS), industrial (IS), and wastewater treatment plant (WWTPS)] were sampled in a 1-year period (January–December 2016) and analyzed for a total of 16 PAHs ($\sum_{16}$PAHs). Sample concentrations measured in this study were reported on the basis of dry weight (DW). The PAH concentrations measured in the branches and needles were 531 ± 281 and 369 ± 256 ng/g DW, 995 ± 643 and 414 ± 265 ng/g DW, 1351 ± 864 and 1047 ± 652 ng/g DW for the SRS, IS, and WWTPS sampling
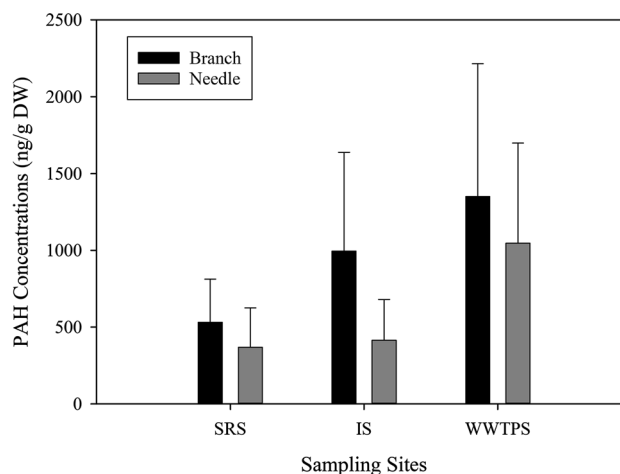
Fig. 2 PAH concentrations in pine needles and pine branches during the sampling period

sites, respectively (Fig. 2). The lowest PAH levels in needles (24–761 ng/g DW) and branches (163–981 ng/g DW) were found in the semi-rural site because this region was relatively remote to the local PAH sources. PAH levels in pine needles (120–1018 ng/g DW) and branches (382–2178 ng/g DW) in the industrial zone were higher than in the rural areas. The wastewater treatment plant site had higher PAH levels in pine needles (142–2565 ng/g DW) and branches (139–2871 ng/g DW) than other sampling sites. In similar studies, PAH concentrations in pine needles were determined as 88.8–692 ng/g DW in background regions and 654–12,161 ng/g DW in industrial zones (Ozgunerge Falay et al. 2013). The values found in this study were in line with the results reported from the similar regions (Lehndorff and Schwark 2004; Piccardo et al. 2005; Ratola et al. 2009; Tomashuk et al. 2012; Ozgunerge Falay et al. 2013; Odabasi et al. 2015) (Table 1). The sampling point in the wastewater treatment plant was from a pine tree near the lagoons, where the treated sludge was stored. PAH concentrations have been found at the highest level since sewage sludges concentrate semivolatile organic compounds, such as PAH (Salihoglu et al. 2012; Wołejko et al. 2018). PAH levels in the SRS were higher than rural areas. An important reason for this situation could be the burning of agricultural product residues in the SRS. In a study by Agarwal et al. (2009), it was stated

that open burning of agricultural products in rural areas resulted in incomplete combustion and consequently low molecular weight PAHs. In addition, diesel fuels, which are commonly used in various agricultural applications, cause PAH concentrations in these regions (Agarwal et al. 2009).

NAP was determined as the most dominant PAH compound (26–56%) in pine branch samples at three sampling sites. NAP was followed by PHE (13–20%), FL (9–24%), FLN (6–14%), and PY (5–10%), respectively (Fig. 3). Moreover, the most dominant type of PAH in the pine needles was NAP (35–52%) followed by PHE (8–19%), FLN (6–15%), FL (7–12%), and CHR (4–8%) (Fig. 3). Similarly, PHE, FLN, PY, and CHR were the dominating compounds in the needle and branch samples in the Iskenderun sampling site (industrial) in Turkey (Ozgunerge Falay et al. 2013). Moreover, PHE, FL, and PY were found to be among the predominant PAHs in pine needles in studies reported from Germany (Lehndorff and Schwark 2004) and Italy (Piccardo et al. 2005). The predominant PAH compounds were found to be the same as the predominant PAH species detected in the ambient air measurement studies conducted in Bursa (Esen et al. 2008; Birgul and Tasdemir 2015).

The atmospheric degradation of the PAHs in the gaseous only proceeds through their reactions with OH radicals (Bedjanian and Nguyen 2010). Due to their semivolatile

Table 1 PAH concentrations in pine needles and pine branches

Concentration (ng/g DW)	Tree component	Characteristic	Place	Date/Period	References
135	Pine needle	Rural	Lencisa, Italy	1997	Piccardo et al. (2005)
101	Pine needle	Traffic			
50	Pine needle	Remote			
153	Pine needle	Urban	Germany	2002	Lehndorff and Schwark (2004)
1773	Pine needle	Rural	Spain	2007	Ratola et al. (2009)
790	Pine needle	Urban			
4187	Pine needle	Urban	USA	2009–2010	Tomashuk et al. (2012)
89–692	Pine needle	Background	Turkey	2010–2011	Ozgunerge Falay et al. (2013)
654–12,161	Pine needle	Industrial			
147 ± 108	Pine branch	Industrial			
358 ± 101	Pine needle (1-year old)	Background	Turkey	2011	Odabasi et al. (2015)
1016 ± 684	Pine needle (1-year old)	Industrial			
509 ± 188	Pine needle (2-year old)	Background			
2157 ± 2098	Pine needle (2-year old)	Industrial			
56 ± 40	Pine branch	Background			
204 ± 193	Pine branch	Industrial			
531 ± 281	Pine branch	Semi-Rural	Turkey	2016	This study
995 ± 643	Pine branch	Industrial			
1351 ± 864	Pine branch	Wastewater treatment			
369 ± 256	Pine needle	Semi-Rural			
414 ± 265	Pine needle	Industrial			
1047 ± 652	Pine needle	Wastewater treatment			

Fig. 3 PAH distribution profiles of pine needles and pine branches in the sites
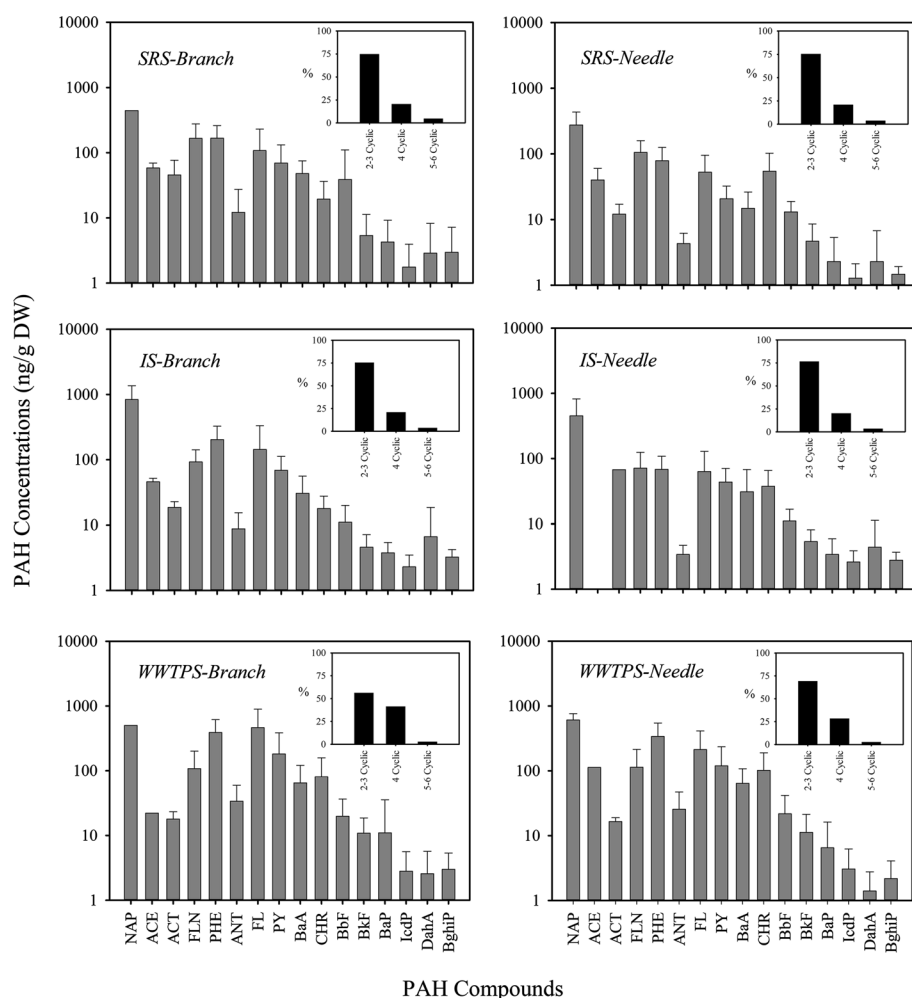
properties, the air-plant exchange is directly or indirectly related to their decomposition by reacting with OH radicals. For this reason, the atmospheric long-range transport of PAHs is less stable than other persistent organic pollutants (POPs) (Cao et al. 2018). For example, ACE and NAP compounds consist of two fused aromatic rings, but ACE has a higher reaction rate than NAP. Similarly, ACT is shown to be more reactive than ACE (Tasdemir and Esen 2007; Keyte et al. 2013). It is indicated that the reactivity of ANT towards OH is much faster than that of other 3-ring PAHs, such as PHE and FLN. ANT, PHE, and FLN have essentially the same 3-ring structure, only differing by the relative position of their aromatic rings (Keyte et al. 2013). However, ANT appears to be more reactive as shown in Fig. 3.

Determination of Regional and Temporal Differences

The coefficient of divergence (COD) method is used to determine the similarities or differences between the PAH concentrations measured in two sampling sites (Bano et al. 2018;

Shen et al. 2019). Another method used to determine the relationship between two sampling sites is the Pearson correlation coefficient (PCC). Usually, COD is used to reflect the degree of variability or similarity of the PAH compounds measured simultaneously in paired sampling sites on a specific day, yet the PCC is used to evaluate the temporal variability of measured PAH compounds (Liu et al. 2017). Basically, the COD and PCC were calculated with the following equations:

$$\text{COD}_{jk} = \sqrt{\frac{1}{p} \sum_{i}^{p} \left(\frac{x_{ij} - x_{ik}}{x_{ij} + x_{ik}} \right)^2} \tag{1}$$

$$\text{PCC}_{jk} = \frac{\sum_{i=1}^{p} \left(x_{ij} - \bar{x}_j \right) x \left(x_{ik} - \bar{x}_k \right)}{\sqrt{\sum_{i=1}^{p} \left(x_{ij} - \bar{x}_j \right)^2 x \sum_{i=1}^{p} \left(x_{ik} - \bar{x}_k \right)^2}} \tag{2}$$

where p is the number of individual PAH congeners, j and k refer to different sampling areas, i is the average concentration of ith PAH congeners, and $\bar{x}$ is the average PAH concentration at sampling areas (Liu et al. 2017; Bano et al.

2018; Chuang et al. 2019; Shen et al. 2019). The PCC and COD values calculated using individual PAH concentrations are used separately or together to understand spatial and temporal changes in pollutant concentrations (Yadav and Turner 2014). If the COD value is above 0.2, there are differences between the sampling sites. Similarly, higher PCC (> 0.7) and lower COD (< 0.2) indicate that not only pollutant sources of two regions are the same, but also they have temporally similar sources (Liu et al. 2017). In this study, COD and PCC results obtained for needles and branches in the sampling areas are shown in Fig. 4.

When the COD values calculated in the winter season were examined, the branch and needle samples belonging to the sampling sites of SRS and IS were smaller than 0.2. These values meant that the pollutant sources in the SRS and IS sampling areas were similar in winter. Because the SRS sampling site referred to a semirural area, there were some agricultural activities in this region. Accordingly, there were emissions from the tractor and heavy vehicles. Similarly, the IS sampling site was close to dense traffic. Probably, the PAH sources due to motor vehicle emissions in these two regions showed similarities in the possible sources. In addition, the PCC values calculated in the winter season indicated a temporal similarity in the sampling media except for the SRS and WWTPS branch and the SRS and IS needle samples. In the spring and autumn seasons, the PCC values calculated for all sampling media were higher than 0.7, indicating that there was no temporal difference between sampling media in these seasons. In the summer season, the COD (> 0.2) and PCC (< 0.7) values calculated in the SRS-WWTPS and the SRS-IS branch samples showed differences in both temporal variations and pollutant sources. The COD and PCC methods can be employed only to determine whether the sources are similar and to determine whether they change temporarily or not. Therefore, methods, such as diagnostic ratios (DRs), ring profile, and principal component analysis (PCA), were

employed in this study to determine possible PAH sources in a more definite manner.

## Source Identification of PAHs

Diagnostic Ratios of PAHs

The distribution of PAH compounds may vary depending on emission sources (Dat and Chang 2017). In many studies, the molecular diagnostic ratios (DRs) are used to determine the sources of PAHs, including domestic sources, mobile sources, industrial, and agricultural sources. However, each of the diagnostic approaches has its limitations and uncertainties. Different diagnostic rates are used to differentiate PAHs that are formed by the petrogenic (volatilization from liquid fuels) and pyrolytic (combustion of fuels) sources (Duodu et al. 2017). For example, ANT is more unstable than PHE. ANT/(ANT + PHE) ratio is generally used to determine the sources of oil and combustion. It refers to oil resources if this ratio is < 0.1, but if this ratio is > 0.1, it indicates the sources of combustion (Yunker et al. 2002; Gong et al. 2018). The FL/(FL + PY) ratio is generally used to evaluate biomass combustion. FL/(FL + PY) ratio > 0.5 means that emissions are affected by the combustion of coal and biomass, yet the ratio < 0.5 refers to the combustion of petroleum fuels (Tobiszewski and Namieśnik 2012; Choi 2014; Hanedar et al. 2014). If the FL/(FL + PY) ratio is between 0.4 and 0.5, it characterizes the sources arising from the combustion of liquid fossil fuels (crude oil and vehicle). In addition, this term liquid fuel refers to mixed sources (Bu et al. 2009). At last, the ratio of BaA/(BaA + CHR) under 0.2 indicates that the sources of PAHs are raised from petroleum combustion, between 0.2 and 0.35 it is from mixed sources, and above 0.35, it is originated from biomass and coal combustions (Yunker et al. 2002; Tobiszewski and Namieśnik 2012; Baniemam et al. 2017). The seasonal diagnostic ratios, obtained in this study, are shown in Fig. 5.
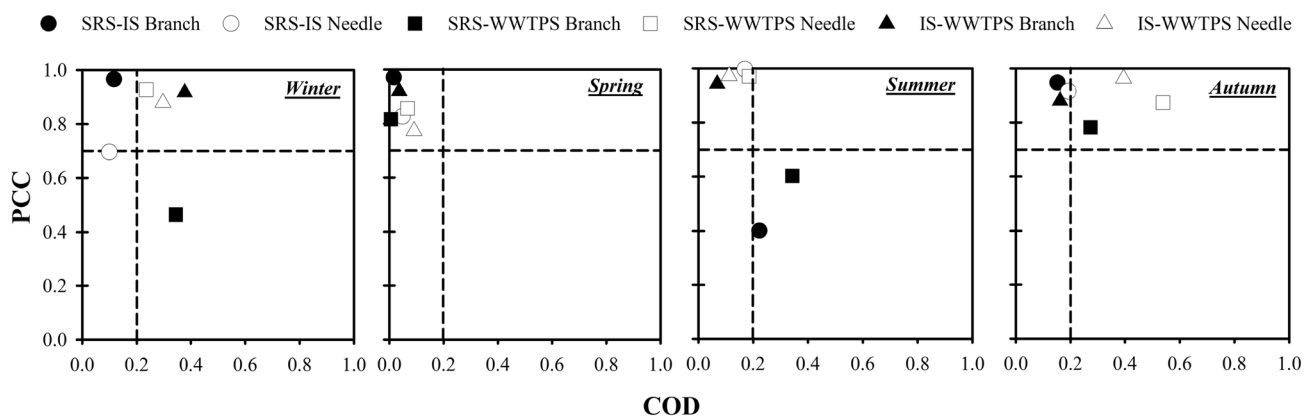
Fig. 4 The coefficient of divergence (COD) versus the Pearson correlation coefficient (PCC)

Fig. 5 Diagnostic ratios of PAHs for the sampling sites
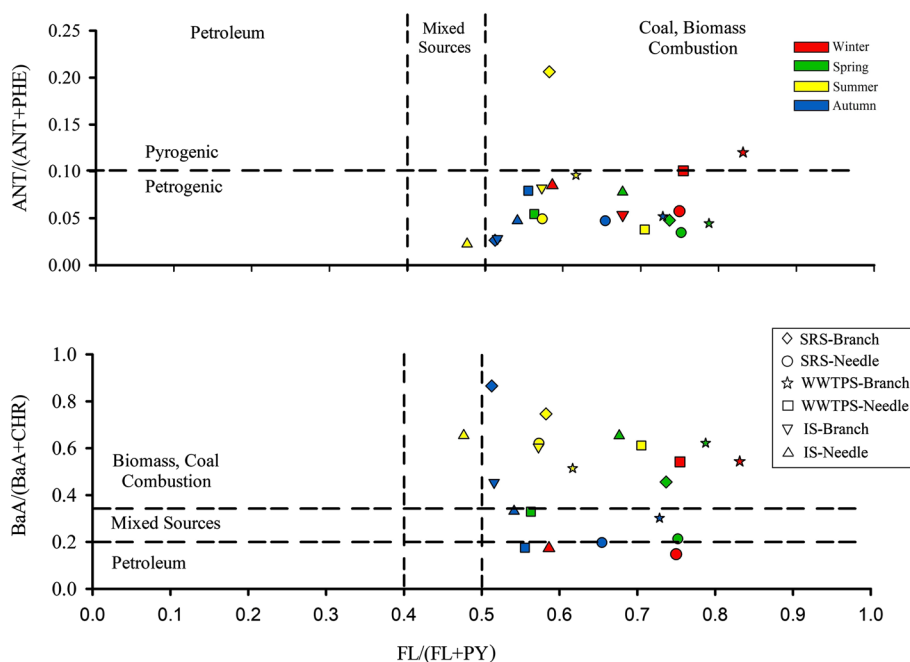
The ANT/(ANT + PHE) ratio is generally < 0.1 in all seasons. Furthermore, the ANT/(ANT + PHE) ratio is highly affected by photoreactivity. The ratio of ANT/(ANT + PHE) is very close to 0 (Tobiszewski and Namieśnik 2012). Based on this information, the samples could be affected by photoreaction with the petrogenic source. BaA/(BaA + CHR) and FL/(FL + PY) ratios generally indicated that samples were influenced by biomass and coal combustion.

ANT/(ANT + PHE), FL/(FL + PY), and BaA/(BaA + CHR) ratios obtained in this study were in line with the ratios obtained from other studies (Hwang et al. 2003; Orecchio et al. 2008; Sun et al. 2010; Choi 2014; De Nicola et al. 2017) (Table 2). High FL/(FL + PY) ratio was found in the branch and needle samples taken from the SRS and WWTPS. In a study by Choi (2014), high FL/(FL + PY) ratio was reported due to biomass burning. In addition, FL, PY, and CHR characterize more coal-burning sources with biomass (Cetin et al. 2018). The branches and needles of the IS sampling site generally had smaller FL/(FL + PY) ratios compared with other regions. Less FL/(FL + PY) ratios suggested the mixed sources in this region (Tobiszewski and Namieśnik 2012; Choi 2014).

Atmospheric conditions affect the dispersion of pollutants (Tobiszewski and Namieśnik 2012). In general, steady weather, low temperature, and thermal inversion in winter generally limit the distribution and transport of pollutants (Tripathi et al. 1996). As a result, increases in concentrations are observed. In addition, this situation becomes more complex by the strong influence of sources including residential heating (Tobiszewski and Namieśnik 2012; Liu et al. 2018). Therefore, the effects of emissions from the sources at different distances to the sampling site would be masked and the diagnostic ratio results mislead.

Ring Profile of PAHs

The molecular weight distributions of the PAH concentrations measured during the sampling period are shown in Table 3. PAHs are taken into the plant tissues through the roots, especially in plants exposed to contaminated soils (Oguntimehin et al. 2010). On the other hand, PAH pollution in the atmosphere generally reaches the plants by precipitation of the particle phase onto the upper layers of the leaves or by keeping the gas phase in the stoma (Kipopoulou et al. 1999; Oguntimehin et al. 2010). The highly found PAH compound was NAP in all sampling sites and tree components (Table 3). In various studies in the literature, the atmospheric NAP has been reported as dominant species (Fang et al. 2004; Lai et al. 2017). The low molecular weight (LMW) PAHs, especially NAP, mainly existed in the gaseous phase, and also the sources of NAP were primarily from biomass burning and fuel combustion (Lai et al. 2017). Among the medium MW PAHs, FL appeared to be the predominant species (Table 3). FL is an indicator of heavy-duty diesel combustion (Khuman et al. 2018). BbF, a high MW PAH, was found to be the dominant compound in the samples (Table 3). BbF is reported among the most significant HMW PAHs emitted from coal combustion (Zhang et al. 2014). In addition, fossil fuel burning and some heating systems cause high BbF concentrations (Arhami et al. 2018).

Table 2 Diagnostic ratios of PAHs in pine components

Ratios		Species	Place	Date	References
ANT/(ANT+PHE)	0.027	Needles	Mexico, Rural/Industrial Area	1999	Hwang et al. (2003)
FL/(FL+PY)	0.362				
BaA/(BaA+CHR)	0.189				
ANT/(ANT+PHE)	0.079	Needles	Spain, Rural	1999	De Nicola et al. (2017)
FL/(FL+PY)	0.644				
BaA/(BaA+CHR)	0.218				
ANT/(ANT+PHE)	0.045	Bark	Italy, Palermo (City Centre)	From 2004 to 2005	Orecchio et al. (2008)
FL/(FL+PY)	0.493				
BaA/(BaA+CHR)	0.072				
ANT/(ANT+PHE)	0.182	Needles	Poland, Forest	2008	Sun et al. (2010)
FL/(FL+PY)	0.337				
BaA/(BaA+CHR)	0.654				
ANT/(ANT+PHE)	0.102	Bark	South Korea, Forest Fire Area (1-Month)	2014	Choi (2014)
FL/(FL+PY)	0.865				
BaA/(BaA+CHR)	0.390				
ANT/(ANT+PHE)	0.052	Needles	Semi-Rural Site (SRS)	2016	This study
FL/(FL+PY)	0.718				
BaA/(BaA+CHR)	0.214				
ANT/(ANT+PHE)	0.068	Branch			
FL/(FL+PY)	0.609				
BaA/(BaA+CHR)	0.712				
ANT/(ANT+PHE)	0.047	Needles	Industrial Site (IS)	2016	This study
FL/(FL+PY)	0.592				
BaA/(BaA+CHR)	0.451				
ANT/(ANT+PHE)	0.041	Branch			
FL/(FL+PY)	0.675				
BaA/(BaA+CHR)	0.632				
ANT/(ANT+PHE)	0.070	Needles	Wastewater Treatment Site (WWTPS)	2016	This study
FL/(FL+PY)	0.641				
BaA/(BaA+CHR)	0.387				
ANT/(ANT+PHE)	0.080	Branch			
FL/(FL+PY)	0.712				
BaA/(BaA+CHR)	0.447				

Principal Component Analysis of PAHs

Principal component analysis (PCA) is a statistical analysis method that converts a data set into several important explanatory factors or principal components (PCs) that meet most of the variance and emphasize the most important information of the original data (Nguyen et al. 2018). According to this analysis method, PAHs can be interpreted according to the PCs forming emission sources. However, the nondiscernibility of the emission sources is shown as a disadvantage of PCA (Cesari et al. 2018; Nguyen et al. 2018).

According to the results of PCA, PC1 compounds for all sampling sites explained 29.47–58.60% of the data (Table S2a–f) (Supplementary Materials). The predominant species identified in PC1 were FL and PY for pine tree components [Factor loading > 0.6 (Kurre et al. 2010)]. FL and PY characterize emissions from diesel and biodiesel fuels (Tipmanee et al. 2012; Dat and Chang 02017). BbF, BkF, and IcdP were the other dominant components of PC1 for branches and needles in SRS and WWTPS sampling sites. BkF characterizes emissions from biomass combustion (Taghvaee et al. 2018), whereas BbF and IcdP indicate the emissions from the combustion of fossil fuels (Arhami et al. 2018; Zhang et al. 2014). Finally, ANT was another dominant compound in PC1, measured in the needles in all sampling sites. ANT characterizes pollution from diesel engine emissions (Zhang et al. 2019).

PC2 referred to 14.17–26.03% of data (Table S2a–f). NAP was the dominant compound for SRS-N (N: needle),

Table 3 Molecular weight distributions of the PAH

PAHs (ng/g DW)		SRS		WWTPS		IS	
		Needles	Branches	Needles	Branches	Needles	Branches
NAP	Low molecular weight	**276.46**	**443.62**	609.27	501.54	453.75	836.43
ACE		40.23	58.44	112.82	22.13	–	46.00
ACY		12.13	45.48	16.43	17.95	67.68	18.60
FLN		105.66	166.08	113.45	107.73	71.38	92.46
PHE		78.77	167.40	338.87	389.52	68.32	203.22
ANT		4.31	12.18	25.56	33.94	3.41	8.80
FL	Medium molecular weight	52.80	**107.80**	212.45	463.42	**63.18**	**143.51**
PY		20.75	69.30	119.25	182.00	43.62	68.98
BaA		14.84	47.89	64.11	65.16	30.95	30.66
CHR		**54.66**	19.40	101.61	80.52	37.66	17.86
BbF	High molecular weight	**13.09**	**38.88**	**21.74**	**19.79**	**11.06**	**11.06**
BkF		4.68	5.37	11.22	10.84	5.36	4.59
BaP		2.29	4.27	6.50	10.97	3.40	3.78
IcdP		1.28	1.76	3.05	2.80	2.61	2.29
DahA		2.30	2.88	1.40	2.57	4.41	6.66
BghiP		1.47	2.97	2.18	2.99	2.78	3.25

Bold character shows maximum concentration levels in that group of PAHs

IS-B (B: branch), and IS-N. It particularity characterizes the emissions generated during the combustion of the biomass (Lai et al. 2017). ACT and FLN were the dominant species for SRS-B. These compounds were originated from wood-burning and heavy-duty diesel combustion (Tipmanee et al. 2012; Lai et al. 2017; Khuman et al. 2018). The SRS-B region was a semirural area where the trees/woods were used for heating. In addition, olive tree branches and leaves in this region were destroyed by burning after pruning. Tractors and other motor vehicles caused diesel emissions. Similarly, other dominant compounds in PC2 were the high molecular weight PAHs. These compounds played a role in determining the emissions generated by the use of fossil fuels (Arhami et al. 2018; Zhang et al. 2014).

The dominant compounds in PC3 for SRS-N, WWTPS-B, IS-B, and IS-N were the PAHs having LMW (Table S2a–f). These compounds characterized emissions from burning biomass (Lai et al. 2017). The dominant species in PC3 for SRS-B was CHR, whereas the dominant species in PC3 for WWTPS-N was NAP. CHR is used to determine the emissions generated during the incomplete combustion of carbon-rich fuels (Eccleshare et al. 2017). NAP is used as an indicator compound for the determination of emissions from traffic (Lai et al. 2017; Taghvaee et al. 2018) while determining the emissions generated from the combustion of biomass and petrogenic sources (Taghvaee et al. 2018).

In other regions except for SRS-N, PC4 was the main component. PC4 referred to 7.49–15.80% of the data (Table S2a–f). The predominant compounds were not determined for SRS-B and WWTPS-N with PC4 [Factor loading < 0.6 (Kurre et al. 2010)]. NAP and BaP were the dominant species for IS-N and WWTPS-B, PHE dominated in IS-N, and DahA was the predominant species in IS-B. BaP is generally used to detect emissions during wood burning, whereas NAP and PHE are used to determine petrogenic sources (Taghvaee et al. 2018). PC5 was determined as the main component in the branch media of all sampling sites (Table S2a–f). The dominant compounds were NAP and DahA in SRS-B and WWTPS-B, respectively. In IS-B, a dominant compound could not be identified (Factor loading < 0.6).

Conclusions

In this study, PAH levels were determined with the help of the pine tree branch (B) and needle (N) collected from three different sites for a 1-year period. The lowest annual PAH concentration was observed in the branches and needles of the semirural site away from the local PAH sources, and the highest annual PAH concentrations were observed in the needles and branches sampled from the city wastewater treatment plant site. The results reported here were in line with the ones reported in the literature. On average, lower PAH levels were measured in the pine needles, whereas higher concentrations were found in the pine branches.

Traditional and statistical methods such as diagnostic ratio (DR), ring profile, the coefficient of divergence (COD), the Pearson correlation coefficient (PCC), and principal component analysis (PCA) were used successfully to define the sources of PAHs. According to the COD values, the PAH sources in the SRS-IS sampling areas were similar in winter.

Results of the PCC values in the spring and autumn seasons, there was no temporal difference between sampling media in these seasons. In the summer season, in the SRS-WWTPS and SRS-IS branch samples showed differences in both temporal variations and pollutant sources. A conclusion can be made that pine tree components could give information about atmospheric PAH concentrations and their sources.

References

Agarwal T, Khillare PS, Shridhar V, Ray S (2009) Pattern, sources and toxic potential of PAHs in the agricultural soils of Delhi, India. J Hazard Mater 163:1033–1039. https://doi.org/10.1016/j.jhazmat.2008.07.058

Agudelo-Castañeda DM, Teixeira EC (2014) Seasonal changes, identification and source apportionment of PAH in PM1.0. Atmos Environ 96:186–200. https://doi.org/10.1016/j.atmosenv.2014.07.030

Arhami M, Shahne MZ, Hosseini V, Roufigar Haghighat N, Lai AM, Schauer JJ (2018) Seasonal trends in the composition and sources of PM2.5 and carbonaceous aerosol in Tehran, Iran. Environ Pollut 239:69–81. https://doi.org/10.1016/j.envpol.2018.03.111

Baniemam M, Moradi AM, Bakhtiari AR, Fatemi MR, Khanghah KE (2017) Seasonal variation of polycyclic aromatic hydrocarbons in the surface sediments of the southern Caspian Sea. Mar Pollut Bull 117:478–485. https://doi.org/10.1016/j.marpolbul.2017.01.027

Bano S, Pervez S, Chow JC, Matawle JL, Watson JG, Sahu RK, Srivastava A, Tiwari S, Pervez YF, Deb MK (2018) Coarse particle (PM10–2.5) source profiles for emissions from domestic cooking and industrial process in Central India. Sci Total Environ 627:1137–1145. https://doi.org/10.1016/j.scitotenv.2018.01.289

Bedjanian Y, Nguyen ML (2010) Kinetics of the reactions of soot surface-bound polycyclic aromatic hydrocarbons with O3. Chemosphere 79:387–393. https://doi.org/10.1016/j.chemosphere.2010.02.009

Birgul A, Tasdemir Y (2015) Concentrations, gas-particle partitioning, and seasonal variations of polycyclic aromatic hydrocarbons at four sites in Turkey. Arch Environ Contam Toxicol 68:46–63. https://doi.org/10.1007/s00244-014-0105-8

Bu QW, Zhang ZH, Lu S, He FP (2009) Vertical distribution and environmental significance of PAHs in soil profiles in Beijing, China. Environ Geochem Health 31:119–131. https://doi.org/10.1007/s10653-008-9171-z

Cao S, Na G, Li R, Ge L, Gao H, Jin S, Hou C, Gao Y, Zhang Z (2018) Fate and deposition of polycyclic aromatic hydrocarbons in the Bransfield Strait, Antarctica. Mar Pollut Bull 137:533–541. https://doi.org/10.1016/j.marpolbul.2018.10.045

Cesari D, De Benedetto GE, Bonasoni P, Busetto M, Dinoi A, Merico E, Chirizzi D, Cristofanelli P, Donateo A, Grasso FM, Marinoni A, Pennetta A, Contini D (2018) Seasonal variability of PM2.5 and PM10 composition and sources in an urban background site in Southern Italy. Sci Total Environ 612:202–213. https://doi.org/10.1016/j.scitotenv.2017.08.230

Cetin B, Yurdakul S, Gungormus E, Ozturk F, Sofuoglu SC (2018) Source apportionment and carcinogenic risk assessment of passive air sampler-derived PAHs and PCBs in a heavily industrialized region. Sci Total Environ 633:30–41. https://doi.org/10.1016/j.scitotenv.2018.03.145

Cheng LH, Yeh CF, Tsai KC, Lee PF, Tseng TP, Huang LJ, Yeh SH, Hsu HT, Lin CH, Lai CH, Brimblecombe P, Chen MJ (2019) Effect of pool fire scale of heavy fuel oil on the characteristics of PAH emissions. Fuel 235:933–943. https://doi.org/10.1016/j.fuel.2018.08.022

Choi SD (2014) Time trends in the levels and patterns of polycyclic aromatic hydrocarbons (PAHs) in pine bark, litter, and soil after a forest fire. Sci Total Environ 470–471:1441–1449. https://doi.org/10.1016/j.scitotenv.2013.07.100

Chuang H-C, Sun J, Ni H, Tian J, Lui KH, Han Y, Cao J, Huang R-J, Shen Z, Ho K-F (2019) Characterization of the chemical components and bioreactivity of fine particulate matter produced during crop-residue burning in China. Environ Pollut 245:226–234. https://doi.org/10.1016/j.envpol.2018.10.119

Cindoruk SS, Esen F, Tasdemir Y (2005) Concentration and gas/particle partitioning of polychlorinated biphenyls (PCBs) at an industrial site at Bursa, Turkey. Atmos Res 85:338–350. https://doi.org/10.1016/j.atmosres.2007.02.004

Dat ND, Chang MB (2017) Review on characteristics of PAHs in atmosphere, anthropogenic sources and control technologies. Sci Total Environ 609:682–693. https://doi.org/10.1016/j.scitotenv.2017.07.204

De Nicola F, Concha Graña E, López Mahía P, Muniategui Lorenzo S, Prada Rodríguez D, Retuerto R, Carballeira A, Aboal JR, Fernández JÁ (2017) Evergreen or deciduous trees for capturing PAHs from ambient air? A case study. Environ Pollut 221:276–284. https://doi.org/10.1016/j.envpol.2016.11.074

Duodu GO, Ogogo KN, Mummullage S, Harden F, Goonetilleke A, Ayoko GA (2017) Source apportionment and risk assessment of PAHs in Brisbane River sediment, Australia. Ecol Indic 73:784–799. https://doi.org/10.1016/j.ecolind.2016.10.038

Eccleshare L, Selzer S, Woodward S (2017) An efficient synthesis of substituted chrysenes. Tetrahedron Lett 58:393–395. https://doi.org/10.1016/j.tetlet.2016.12.004

Esen F, Cindoruk SS, Taşdemir Y (2006) Ambient concentrations and gas/particle partitioning of polycyclic aromatic hydrocarbons in an urban site in Turkey. Environ Forensics 7:303–312. https://doi.org/10.1080/15275920600996099

Esen F, Tasdemir Y, Vardar N (2008) Atmospheric concentrations of PAHs, their possible sources and gas-to-particle partitioning at a residential site of Bursa, Turkey. Atmos Res 88:243–255. https://doi.org/10.1016/j.atmosres.2007.11.022

Fang GC, Chang KF, Lu C, Bai H (2004) Estimation of PAHs dry deposition and BaP toxic equivalency factors (TEFs) study at Urban, Industry Park and rural sampling sites in central Taiwan, Taichung. Chemosphere 55:787–796. https://doi.org/10.1016/j.chemosphere.2003.12.012

Fang M-D, Lee C-L, Jiang J-J, Ko F-C, Baker JE (2012) Diffusive exchange of PAHs across the air-water interface of the Kaohsiung Harbor lagoon, Taiwan. J Environ Manag 110:179–187. https://doi.org/10.1016/j.jenvman.2012.06.001

Gong X, Xiao L, Zhao Z, Li Q, Feng F, Zhang L, Deng Z (2018) Spatial variation of polycyclic aromatic hydrocarbons (PAHs) in surface sediments from rivers in hilly regions of Southern China in the wet and dry seasons. Ecotoxicol Environ Saf 156:322–329. https://doi.org/10.1016/j.ecoenv.2018.03.004

Günindi M, Tasdemir Y (2010) Atmospheric polychlorinated biphenyl (pcb) inputs to a coastal city near the marmara sea. Mar Pollut Bull 60:2242–2250. https://doi.org/10.1016/j.marpolbul.2010.08.012

Hanedar A, Alp K, Kaynak B, Avşar E (2014) Toxicity evaluation and source apportionment of Polycyclic Aromatic Hydrocarbons (PAHs) at three stations in Istanbul, Turkey. Sci Total Environ 488–489:437–446. https://doi.org/10.1016/j.scitotenv.2013.11.123

Howsam M, Jones KC, Ineson P (2000) PAH associated with the leaves of three deciduous tree speciesI.pdf. 108

Hwang HM, Wade TL, Sericano JL (2003) Concentrations and source characterization of polycyclic aromatic hydrocarbons in pine needles from Korea, Mexico, and United States. Atmos Environ 37:2259–2267. https://doi.org/10.1016/S1352-2310(03)00090-6

Keyte IJ, Harrison RM, Lammel G (2013) Chemical reactivity and long-range transport potential of polycyclic aromatic hydrocarbons—a review. Chem Soc Rev 42:9333–9391. https://doi.org/10.1039/c3cs60147a

Khuman SN, Chakraborty P, Cincinelli A, Snow D, Kumar B (2018) Polycyclic aromatic hydrocarbons in surface waters and riverine sediments of the Hooghly and Brahmaputra Rivers in the Eastern and Northeastern India. Sci Total Environ 636:751–760. https://doi.org/10.1016/j.scitotenv.2018.04.109

Kipopoulou AM, Manoli E, Samara C (1999) Bioconcentration of polycyclic aromatic hydrocarbons in vegetables grown in an industrial area Bioconcentration of polycyclic aromatic hydrocarbons in vegetables grown in an industrial area. Environ Pollut 106:369–380. https://doi.org/10.1016/S0269-7491(99)00107-4

Kurre A, Bastiaenen CHG, Van Gool CJAW, Gloor-Juzi T, De Bruin ED, Straumann D (2010) Exploratory factor analysis of the Dizziness Handicap Inventory (German version). BMC Ear Nose Throat Disord 10:1–10. https://doi.org/10.1186/1472-6815-10-3

Kuzu SL (2016) Compositional variation of PCBs, PAHs, and OCPs at gas phase and size segregated particle phase during dust incursion from the saharan desert in the northwestern anatolian peninsula. Adv Meteorol. https://doi.org/10.1155/2016/7153286

Lai YC, Tsai CH, Chen YL, Chang-Chien GP (2017) Distribution and sources of atmospheric polycyclic aromatic hydrocarbons at an industrial region in Kaohsiung, Taiwan. Aerosol Air Qual Res 17:776–787. https://doi.org/10.4209/aaqr.2016.11.0482

Lehndorff E, Schwark L (2004) Biomonitoring of air quality in the cologne conurbation using pine needles as a passive sampler—Part II: polycyclic aromatic hydrocarbons (PAH). Atmos Environ 38:3793–3808. https://doi.org/10.1177/1356766705052569

Li L, Lu Y, Shi Y, Wang T, Luo W, Gosens J, Chen P, Li H (2013) Integrated technology selection for energy conservation and PAHs control in iron and steel industry: methodology and case study. Energy Policy 54:194–203. https://doi.org/10.1016/j.enpol.2012.11.022

Liu JJ, Wang XC, Fan B (2011) Characteristics of PAHs adsorption on inorganic particles and activated sludge in domestic wastewater treatment. Bioresour Technol 102:5305–5311. https://doi.org/10.1016/j.biortech.2010.12.063

Liu Y, Yan C, Ding X, Wang X, Fu Q, Zhao Q, Zhang Y, Duan Y, Qiu X, Zheng M (2017) Sources and spatial distribution of particulate polycyclic aromatic hydrocarbons in Shanghai, China. Sci Total Environ 584–585:307–317. https://doi.org/10.1016/j.scitotenv.2016.12.134

Liu Y, Yu Y, Liu M, Lu M, Ge R, Li S, Liu X, Dong W, Qadeer A (2018) Characterization and source identification of PM2.5-bound polycyclic aromatic hydrocarbons (PAHs) in different seasons from Shanghai, China. Sci Total Environ 644:725–735. https://doi.org/10.1016/j.scitotenv.2018.07.049

Malawska M, Ekonomiuk A, Wilkomirski B (2006) Polycyclic aromatic hydrocarbons in peat cores from southern Poland: distribution in stratigraphic profiles as an indicator of PAH sources. Environ Monit Assess 1:1–14. https://doi.org/10.1590/S1516-05722010000400005

Mętrak M, Aneta E, Wiłkomirski B, Staszewski T, Suska-Malawska M (2016) Interspecific differences in foliar 1 PAHs load between Scots pine, birch, and wild rosemary from three polish peat bogs. Environ Monit Assess 188:1–13. https://doi.org/10.1007/s10661-016-5465-2

Nguyen TNT, Jung KS, Son JM, Kwon HO, Choi SD (2018) Seasonal variation, phase distribution, and source identification of atmospheric polycyclic aromatic hydrocarbons at a semi-rural site in Ulsan, South Korea. Environ Pollut 236:529–539. https://doi.org/10.1016/j.envpol.2018.01.080

Odabasi M, Ozgunerge Falay E, Tuna G, Altiok H, Kara M, Dumanoglu Y, Bayram A, Tolunay D, Elbir T (2015) Biomonitoring the spatial and historical variations of persistent organic pollutants (POPs) in an industrial region. Environ Sci Technol 49:2105–2114. https://doi.org/10.1021/es506316t

Oguntimehin I, Eissa F, Sakugawa H (2010) Negative effects of fluoranthene on the ecophysiology of tomato plants (Lycopersicon esculentum Mill). Fluoranthene mists negatively affected tomato plants. Chemosphere 78:877–884. https://doi.org/10.1016/j.chemosphere.2009.11.030

Oishi Y (2013) Comparison of pine needles and mosses as bio-indicators for polycyclic aromatic hydrocarbons. J Environ Prot (Irvine, Calif) 04:106–113. https://doi.org/10.4236/jep.2013.48A1013

Orecchio S, Gianguzza A, Culotta L (2008) Absorption of polycyclic aromatic hydrocarbons by Pinus bark: analytical method and use for environmental pollution monitoring in the palermo area (Sicily, Italy). Environ Res 107:371–379. https://doi.org/10.1016/j.envres.2008.02.010

Ozaki N, Takamura Y, Kojima K, Kindaichi T (2015) Loading and removal of PAHs in a wastewater treatment plant in a separated sewer system. Water Res 80:337–345. https://doi.org/10.1016/j.watres.2015.05.002

Ozcan S, Aydin ME (2009) Polycyclic aromatic hydrocarbons, polychlorinated biphenyls and organochlorine pesticides in urban air of Konya, Turkey. Atmos Res 93:715–722. https://doi.org/10.1016/j.atmosres.2009.02.012

Ozgunerge Falay E, Tuna G, Altiok H, Kara M, Dumanoglu Y, Bayram A, Tolunay D, Elbir T, Odabasi M (2013) Spatial variation of polycyclic aromatic hydrocarbons (PAHs) in air, soil and tree components in iskenderun industrial region, Turkey. Int J Chem Environ Biol Sci 1:263–267

Piccardo MT, Pala M, Bonaccurso B, Stella A, Redaelli A, Paola G, Valerio F (2005) Pinus nigra and Pinus pinaster needles as passive samplers of polycyclic aromatic hydrocarbons. Environ Pollut 133:293–301. https://doi.org/10.1016/j.envpol.2004.05.034

Ratola N, Lacorte S, Barceló D, Alves A (2009) Microwave-assisted extraction and ultrasonic extraction to determine polycyclic aromatic hydrocarbons in needles and bark of Pinus pinaster Ait. and Pinus pinea L. by GC-MS. Talanta 77:1120–1128. https://doi.org/10.1016/j.talanta.2008.08.010

Salihoglu NK, Karaca G, Salihoglu G, Tasdemir Y (2012) Removal of polycyclic aromatic hydrocarbons from municipal sludge using UV light. Desalin Water Treat 44:324–333. https://doi.org/10.1080/19443994.2012.691689

Shen R, Liu Z, Chen X, Wang Y, Wang L, Liu Y, Li X (2019) Atmospheric levels, variations, sources and health risk of PM2.5-bound polycyclic aromatic hydrocarbons during winter over the North China Plain. Sci Total Environ 655:581–590. https://doi.org/10.1016/j.scitotenv.2018.11.220

Sun F, Wen D, Kuang Y, Li J, Li J, Zuo W (2010) Concentrations of heavy metals and polycyclic aromatic hydrocarbons in needles of Masson pine (*Pinus massoniana* L.) growing nearby different industrial sources. J Environ Sci 22:1006–1013. https://doi.org/10.1016/S1001-0742(09)60211-4

Taghvaee S, Sowlat MH, Hassanvand MS, Yunesian M, Naddafi K, Sioutas C (2018) Source-specific lung cancer risk assessment of ambient PM2.5-bound polycyclic aromatic hydrocarbons (PAHs) in central Tehran. Environ Int 120:321–332. https://doi.org/10.1016/j.envint.2018.08.003

Tasdemir Y, Esen F (2007) Urban air PAHs: Concentrations, temporal changes and gas/particle partitioning at a traffic site in

Turkey. Atmos Res 84:1–12. https://doi.org/10.1016/j.atmos res.2006.04.003

Tipmanee D, Deelaman W, Pongpiachan S, Schwarzer K, Sompong-chaiyakul P (2012) Using Polycyclic Aromatic Hydrocarbons (PAHs) as a chemical proxy to indicate Tsunami 2004 backwash in Khao Lak coastal area, Thailand. Nat Hazards Earth Syst Sci 12:1441–1451. https://doi.org/10.5194/nhess-12-1441-2012

Tobiszewski M, Namieśnik J (2012) PAH diagnostic ratios for the identification of pollution emission sources. Environ Pollut 162:110–119. https://doi.org/10.1016/j.envpol.2011.10.025

Tomashuk TA, Truong TM, Mantha M, McGowin AE (2012) Atmospheric polycyclic aromatic hydrocarbon profiles and sources in pine needles and particulate matter in Dayton, Ohio, USA. Atmos Environ 51:196–202. https://doi.org/10.1016/j.atmos env.2012.01.028

Torretta V (2012) PAHs in wastewater: Removal efficiency in a conventional wastewater treatment plant and comparison with model predictions. Environ Technol 33:851–855. https://doi.org/10.1080/09593330.2011.599430

Tripathi BD, Chaturvedi SS, Tripathi RD (1996) Seasonal variation in ambient air concentration of nitrate and sulfate aerosols in a tropical city, Varanasi. Atmos Environ 30:2773–2778. https://doi.org/10.1016/1352-2310(95)00435-1

Vardar N, Tasdemir Y, Odabasi M, Noll KE (2004) Characterization of atmospheric concentrations and partitioning of PAHs in the Chicago atmosphere. Sci Total Environ 327:163–174. https://doi.org/10.1016/j.scitotenv.2003.05.002

Wołejko E, Wydro U, Jabłońska-Trypuć A, Butarewicz A, Łoboda T (2018) The effect of sewage sludge fertilization on the concentration of PAHs in urban soils. Environ Pollut 232:347–357. https://doi.org/10.1016/j.envpol.2017.08.120

Yadav V, Turner J (2014) Gauging intraurban variability of ambient particulate matter arsenic and other air toxic metals from a network of monitoring sites. Atmos Environ 89:318–328. https://doi.org/10.1016/j.atmosenv.2014.02.030

Yunker MB, Macdonald RW, Vingarzan R, Mitchell RH, Goyette D, Sylvestre S (2002) PAHs in the Fraser river basin: a critical appraisal of PAH ratios as indicators of PAH source and composition. Org Geochem 33:489–515. https://doi.org/10.1016/S0146-6380(02)00002-5

Zhang P, Wang Y, Yang B, Liu C, Shu J (2014) Heterogeneous reactions of particulate benzo[b]fluoranthene and benzo[k]fluoranthene with NO3 radicals. Chemosphere 99:34–40. https://doi.org/10.1016/j.chemosphere.2013.08.093

Zhang J, Li R, Zhang X, Bai Y, Cao P, Hua P (2019) Vehicular contribution of PAHs in size dependent road dust: a source apportionment by PCA-MLR, PMF, and Unmix receptor models. Sci Total Environ 649:1314–1322. https://doi.org/10.1016/j.scito tenv.2018.08.410